Structural properties of amorphous silicon-carbon films deposited by the filtered cathodic vacuum arc technique

1999 J. Phys.: Condens. Matter 11 5111

(http://iopscience.iop.org/0953-8984/11/26/312)

J. Phys.: Condens. Matter **11** (1999) 5111–5118. Printed in the UK PII: S0953-8984(99)02935-5

Structural properties of amorphous silicon–carbon films deposited by the filtered cathodic vacuum arc technique

J R Shi†, X Shi, Z Sun, E Liu, H S Yang, L K Cheah and X Z Jin

School of Electrical and Electronic Engineering, Nanyang Technological University, Singapore 639798, Singapore

E-mail: ejrshi@ntu.edu.sg

Received 23 March 1999, in final form 11 May 1999

Abstract. Amorphous silicon–carbon films have been successfully deposited by the filtered cathodic vacuum arc technique. The silicon concentration in the films determined by x-ray photoelectron spectroscopy measurement varies from 2.4 to 55 at.%. The structural properties of the films were investigated by using atomic force microscopy, Raman spectroscopy, and x-ray diffraction. All of the films have smooth surface morphology with RMS roughness below 0.6 nm. Both Raman spectroscopy and x-ray diffraction show the existence of silicon carbide clusters in the films with silicon contents between 42 and 48 at.%. The G-peak position of the carbon cluster is shifted to very much lower values of the Raman shift with increasing silicon content. The silicon atoms predominantly substitute for the carbon atoms in the carbon cluster at low silicon content, and form amorphous silicon carbide clusters or amorphous silicon clusters at high silicon content.

1. Introduction

Recently, tetrahedral amorphous carbon (ta-C) film deposited by the filtered cathodic vacuum arc (FCVA) technique has been intensively studied [1–6]. The FCVA deposition system employs a magnetic filtering technique to remove unwanted macro-particles and neutral atoms. Clean ta-C film can be deposited at room temperature. It was shown by electron energy-loss spectroscopy (EELS) that as many as 87% of the carbon atoms in the ta-C film form an amorphous tetrahedral (sp^3) structure [6]. The high sp^3 content in the film results in unique properties that include extreme hardness ($\sim$70 GPa), chemical inertness, high electrical resistivity, and wide optical band gap. Other important factors which make the film an attractive material for coatings include the room temperature deposition, smooth surface and low friction, thermal stability, and transparency over a wide spectral range. But the internal stress of the ta-C film formed during the deposition process is quite high, which has prevented wide application of the ta-C film.

It was reported that incorporation of silicon into amorphous hydrogenated carbon made by the CVD method reduces film stress while maintaining the hardness, friction, and wear [7–9]. Incorporation of other elements, such as boron [10] and nitrogen [11], into ta-C film also reduces the internal stress of the film. This paper presents the structural properties of amorphous silicon–carbon films deposited by the FCVA technique. The mechanical properties of these films will be presented elsewhere. The films were investigated by using x-ray photoelectron spectroscopy (XPS), atomic force microscopy (AFM), micro-Raman spectroscopy, and x-ray

† Author to whom any correspondence should be addressed.

0953-8984/99/265111+08$19.50

diffraction. Amorphous silicon carbide clusters were found in the films with intermediate silicon contents. Structural changes of the films were correlated with the silicon content.

2. Experimental details

The amorphous silicon–carbon films were deposited by a FCVA system described elsewhere [6]. The system incorporates an off-plane double-bend filter [12, 13] to effectively remove all macro-particles. Carbon and silicon ions are produced in a vacuum arc discharge between the cathode and the grounded anode. The cathode is a 60 mm diameter target mounted on a water-cooled stainless-steel block. Pure graphite and silicon powder (325 mesh) with the desired atomic fraction were mixed thoroughly and compressed into a cylindrical target by a pressure of 770 MPa. The arc current was kept constant at 90 A. A toroidal magnetic field of around 40 mT was employed to produce the axial and curvilinear fields to steer the plasma. The deposition rate was kept at about 20 nm min^{-1}, and films with thicknesses between 100 and 120 nm were prepared with the FCVA system in floating conditions at room temperature. The substrate was clean (100) n-type silicon with average thickness 0.5 mm. The native oxide layer on the silicon wafer surface was removed by an argon-ion beam from a RF ion beam source before deposition.

XPS measurement was carried out on a VG Scientific Microlab 310F system using Mg Kα (1253.6 eV) radiation as the x-ray source. All of the XPS spectra of the samples were fitted with Gaussian functions and the background was removed by using a computer program. The elemental composition of the films can be calculated as [14]

$$\%X = \left(\frac{A_X}{S_X}\right) \Big/ \sum_{i=1}^{N} \left(\frac{A_X}{S_X}\right) \tag{1}$$

where X is the element, A_X the area under the peak for element X in the spectrum, and S_X is the sensitivity factor. The sensitivity factors (see p 253 of reference 14) for carbon and silicon are 0.31 and 0.37, respectively. The film surface morphology was observed using the Digital Instruments Dimension 3000 SPM system. An etched silicon cantilever tip with a curvature radius of 10 nm was used for tapping-mode AFM measurement. The root mean square (RMS) roughness was obtained using the digital image-processing package attached to the SPM system over the image area of 1 μm^2. Given that the AFM roughness measurements are very sensitive to both the tip and the surface structure, several tips were used for measurements on the same series of samples and the results are reproducible. The Raman spectra were excited using the 514.5 nm line of an Ar^+ laser and collected with back-scattering on a CCD camera using a Renishaw micro-Raman System 1000 spectrometer. Two multi-layer dielectric filters were used for the rejection of Rayleigh scattering light. A laser output of 20 mW was used, which resulted in an incident power at the sample of approximately 1.5 mW. The high-efficiency 1800 grooves mm^{-1} diffraction grating was used as the single dispersive stage. The spectral range is from 50 to 4000 cm^{-1}, and the spectral resolution is 2.0 cm^{-1} (half-width, half-maximum). X-ray diffraction was performed using the vertical Siemens D5005 x-ray diffractometer. The diffraction was excited by Cu Kα radiation (wavelength of 1.54 Å) at 40 kV and 40 mA. The angle between the incident x-ray and the surface of the films was fixed at 1°, and the diffraction pattern was obtained by changing the position of the counter.

3. Results and discussion

The silicon content in the amorphous silicon–carbon films determined by XPS measurement ranges from 2.4 to 55 at.%. Figure 1 shows the relationship between the silicon atomic fractions

in the film and in the target. The silicon content in the film increases monotonically with the amount of silicon in the target, but the silicon content in the film is always larger than that in the corresponding target. The larger silicon content in the film may result from the lower melting point of silicon compared with graphite. The relationship between the two fractions is not linear, but parabolic. This indicates that the silicon atoms are much easier to introduce into the carbon cluster at low silicon concentration. A similar relationship was found for the nitrogenated ta-C film [11].

All of the amorphous silicon–carbon films exhibit smooth morphology with RMS roughness smaller than 0.6 nm. Figure 2 shows a typical AFM picture of the film with 42 at.% silicon content, and the corresponding RMS roughness is 0.16 nm. The smooth surface morphology of the silicon–carbon films is due to the subimplantation deposition mechanism

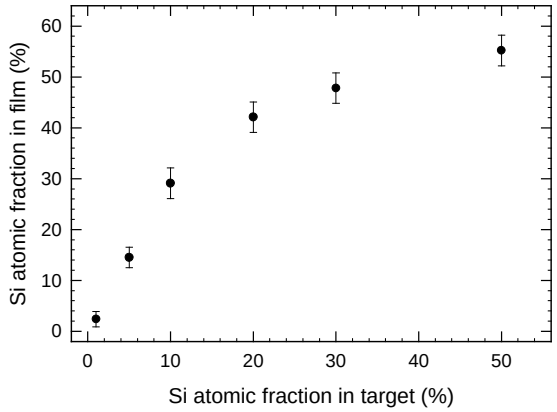

Figure 1. The relationship between the silicon atomic fractions in the film and in the target.

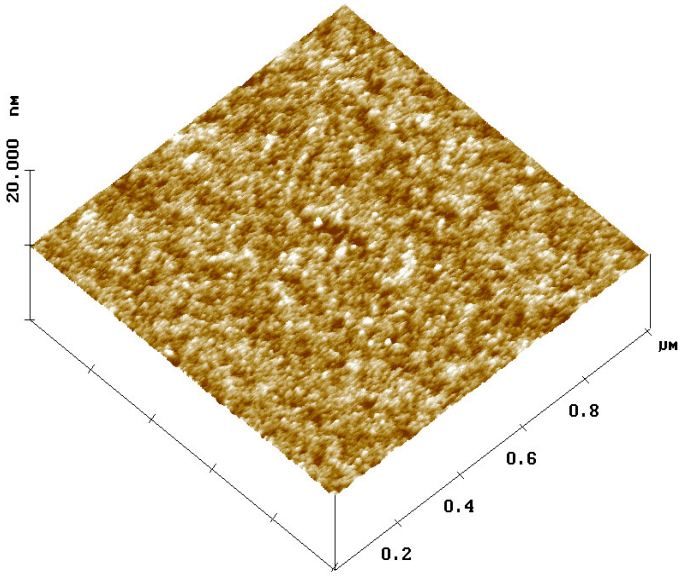

Figure 2. An AFM picture for the amorphous silicon–carbon film with 42 at.% silicon content. The vertical scale is 10 nm/division.

of the FCVA technique [16]. Another reason for the smooth morphology is that an off-plane double-bend filter [12, 13] was used in our FCVA system, by means of which macro-particles and neutral atoms are removed and clean films can be deposited. In the AFM pictures of the silicon–carbon films, a periodic ripple structure is clearly observed. The ripple structure is about 40 nm in width from the cross section analysis. The lateral sizes for the ripple structures for different silicon contents are roughly the same. The explanation for the ripple structure may be that the off-normal-incidence ion bombardment produces periodic height modulations on solid surfaces [15]. This terraced orientation is believed to be critically dependent on the angle of ion beam incidence. The ta-C films deposited by the FCVA technique exhibit smooth morphology depending upon the ion energy. The lowest RMS roughness (0.14 nm) appears at the optimal ion energy for the formation of sp^3-bonded carbon [16].

The Raman spectra for the films with different silicon contents are shown in figure 3 for the range 100 to 2000 cm^{-1}. The spectra have been displaced vertically for clarity. For the films with low silicon contents, a broad band appears in the range 1400–1700 cm^{-1}. This is due to the vibrational mode of the amorphous carbon clusters [17]. A strong narrow peak at 520 cm^{-1} and a wide peak at around 950 cm^{-1} due to the first- and second-order vibrational modes of the silicon substrate, respectively. The appearance of the peaks for the substrate is an indication of the transparency of the film near the laser wavelength of 514.5 nm. For films containing more silicon, a broad band appears at around 800 cm^{-1}, and two broad bands appear at around 480 cm^{-1} and 170 cm^{-1}. The former one resulted from the vibrational mode of the amorphous silicon carbide cluster [18, 19], and the latter two bands are due to the amorphous

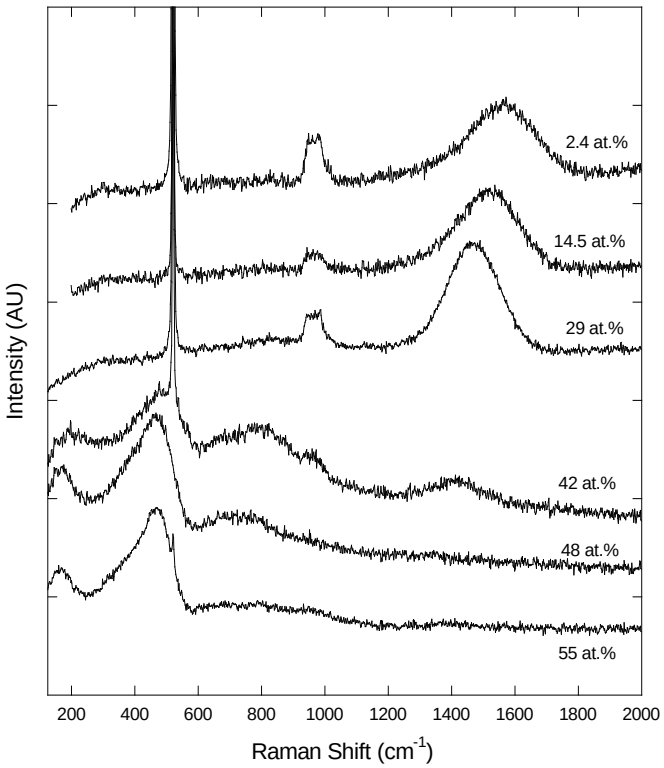

Figure 3. Raman spectra of amorphous silicon–carbon films with different silicon contents.

silicon cluster [20, 21].

The visible Raman spectrum is largely insensitive to the sp^3-bonded component of the carbon cluster [22, 23]. Therefore, the Raman spectrum monitors the state of the sp^2-bonded carbon component within the sp^3 matrix. The broad peak in the range 1400–1700 cm^{-1} was fitted with two Gaussian peaks defined as the disorder ('D') and graphite ('G') peaks, respectively. This notation arises from the Raman spectrum of nanocrystalline graphite, which generally shows two peaks. One peak is due to the in-plane vibrational mode of graphite, and the other is attributable to the small-domain-size graphite region. The fitting for the film containing 2.4 at.% silicon is shown in figure 4. The solid curve is the Gaussian fit to the data points. The broken curves show the decomposed bands. The fitting shows a big G peak and a small D peak. For the films containing 48 and 55 at.% silicon, the Raman band of the carbon cluster becomes very weak and is difficult to identify. Figure 5 shows the G-peak position of the carbon cluster as a function of the silicon concentration. The G position is almost linearly shifted from 1571 cm^{-1} for the film containing 2.4 at.% silicon to 1416 cm^{-1} for the film containing 42 at.% silicon. The great shift of the G position of the carbon cluster is qualitatively explained as follows. At low silicon concentration, the silicon atom predominantly substitutes for the carbon atom. As the atomic fraction of silicon in the film increases, more and more silicon atoms substitute for the carbon atoms in the ring-shaped sp^2-bonded carbon cluster. As the silicon atom is heavier than the carbon atom and the Si–C bond is weaker than the C–C bond, the vibration energy of the stretching mode of the ring becomes lower and lower.

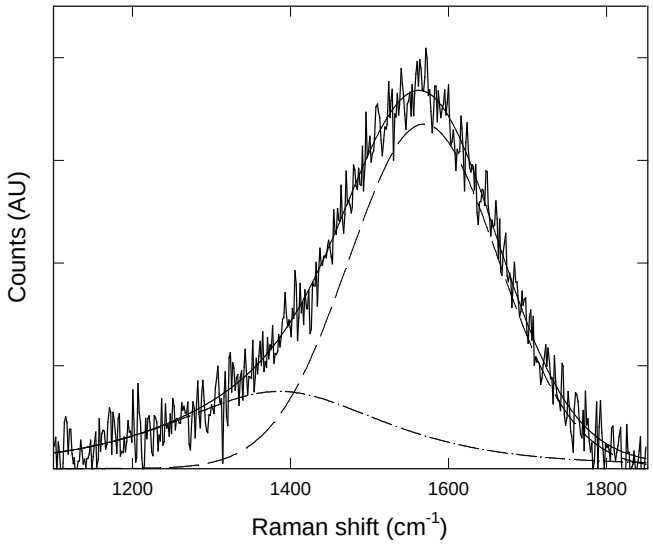

Figure 4. Curve fitting using two Gaussian curves for the carbon cluster. The solid curve shows the fit, and the dashed and dash–dot curves show the individual G and D components of the fit, respectively.

For the film containing 42 at.% silicon, a strong broad peak due to the amorphous silicon carbide cluster appears at 800 cm^{-1}. For the film containing 48 at.% silicon, this peak becomes weak and is centred at 750 cm^{-1}. As the silicon content increases to 55 at.%, there remains a very weak wide peak at around 750 cm^{-1}. The appearance of the wide peak at around 750–800 cm^{-1} suggests that there are separated silicon carbide clusters in these films. IR absorption measurement of amorphous silicon–carbon films deposited by the hot-filament-assisted CVD

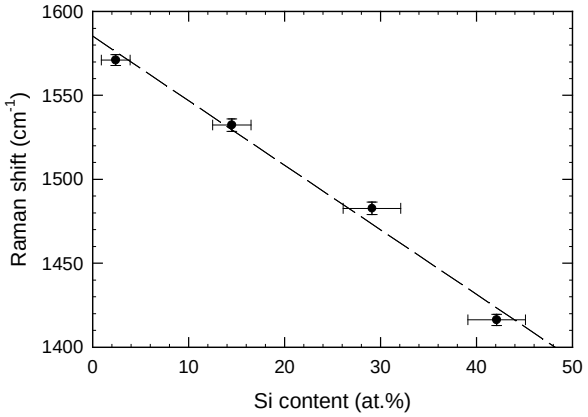

Figure 5. The G-peak position of the carbon cluster versus silicon content.

method [19] showed that the absorption peak corresponding to Si–C vibration shifts from 760 to 800 cm^{-1} as the silicon content decreases. This is in good agreement with our result. The higher peak position for the film with 42 at.% silicon content may result from the amorphous silicon–carbon clusters in the film still being carbon rich.

For the films with silicon concentrations of 42 at.% and above, Raman characterizing modes for amorphous silicon (transverse acoustic (TA) and transverse optical (TO) modes [20]) were observed at around 168 and 480 cm^{-1}, respectively. Figure 6 shows the fitting of the spectrum over the range 125 to 600 cm^{-1} for the film with 48 at.% silicon. The meanings of the solid and broken curves are same as above. The fittings show that a broad longitudinal

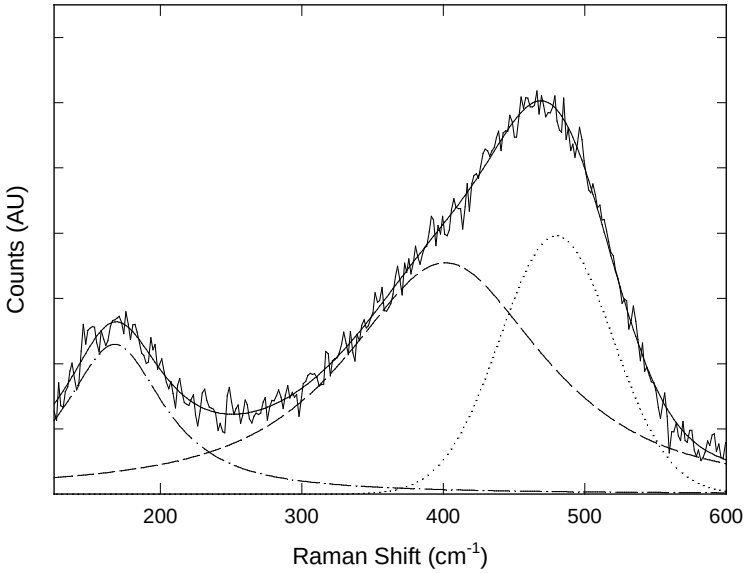

Figure 6. Curve fitting using three Gaussian curves for amorphous silicon clusters. The solid curve shows the fit, and the dotted, dashed, and dash–dot curves show the individual TO, LO, and TA components of the fit.

optical (LO) mode appears at 402 cm^{-1} in addition to the TO mode at 480 cm^{-1} and TA mode at 168 cm^{-1}. As the silicon content increases from 42 at.% to 55 at.%, the Raman shift of the TO mode shifts from 492 to 476 cm^{-1}, while the LO mode and TA mode remain around 400 cm^{-1} and 168 cm^{-1}, respectively. The shift of the peak position of the TO mode indicates that there are some influences of carbon atoms on the amorphous silicon clusters in the films with intermediate silicon contents.

The x-ray diffraction patterns for the films with different silicon contents are shown in figure 7. The strong background on the left-hand side of the diffraction patterns is due to the small angle of incidence used for the measurement. Wide peaks at around 34° were observed for the films with 42 and 48 at.% silicon. For films with low silicon contents, no diffraction peak was observed. This result is similar to that for ta-C film. It is difficult to obtain the diffraction pattern of ta-C film by using x-ray diffraction. For the film with 55 at.% silicon, the wide peak at around 34° disappears. This wide peak at around 34° indicates an amorphous structure, and is considered as a contribution due to amorphous silicon carbide clusters, as the strongest diffraction peak (111) for crystalline silicon carbide is at 35.7° [24]. The x-ray diffraction result is in good agreement with the Raman scattering result that amorphous silicon carbide clusters exist in films with intermediate silicon concentrations.

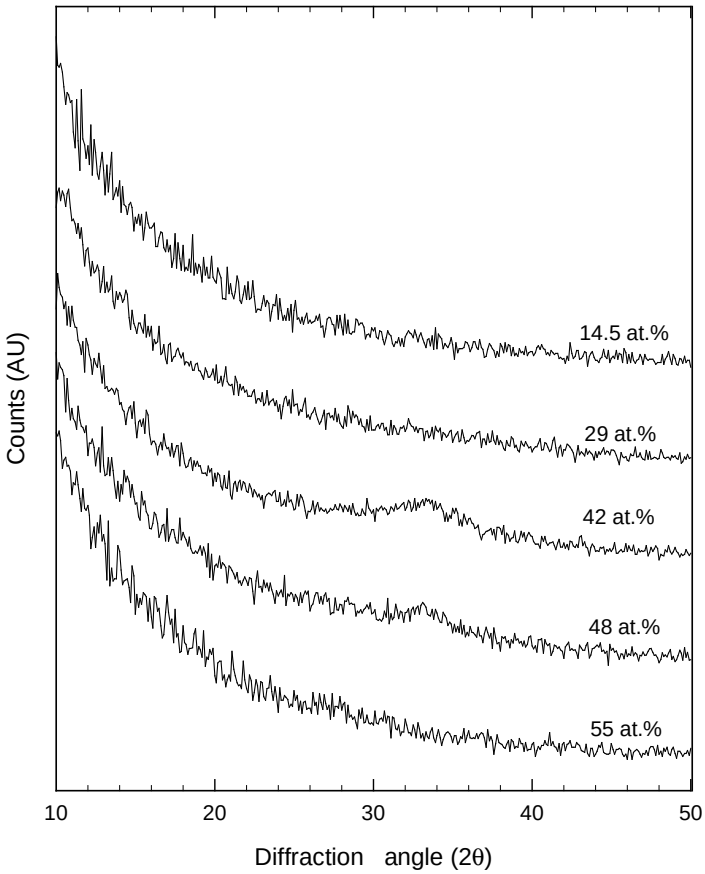

Figure 7. X-ray diffraction patterns of the amorphous silicon–carbon films with different silicon contents.

4. Conclusions

The structural properties of amorphous silicon–carbon films deposited by the FCVA technique were investigated by using atomic force microscopy, Raman spectroscopy, and x-ray diffraction. All of the films have amorphous structure and smooth surface morphology with RMS roughness below 0.6 nm and lateral size around 40 nm. As the silicon content increases, the dominant bonding in the silicon–carbon films changes from C–C bonds to Si–C bonds, and then to Si–Si bonds. The silicon atoms predominantly substitute for the carbon atoms in the amorphous carbon clusters at low silicon concentrations, form amorphous silicon carbide clusters at intermediate silicon concentration, and form amorphous silicon clusters at high silicon concentration.

Acknowledgments

The authors wish to acknowledge the help of Dr Zhang Qing, School of EEE, Nanyang Technological University, for carrying out the x-ray diffraction measurements of the films.

References

[1] Martin P J, Filipczuk S W, Netterfield R P, Field J S, Whitnall D F and McKenzie D R 1988 *J. Mater. Sci. Lett.* **7** 410
[2] Martin P J, Netterfield R P, Kinder T J and Descotes L 1991 *Surf. Coatings Technol.* **49** 239
[3] McKenzie D R, Muller D and Pailthorpe B A 1991 *Phys. Rev. Lett.* **67** 773
[4] Falabella S, Boercker D B and Sanders D M 1993 *Thin Solid Films* **236** 82
[5] Fallon P J, Veerasamy V S, Davis C A, Robertson J, Amaratunga G A J, Milne W I and Koskinen J 1993 *Phys. Rev.* B **48** 4777
[6] Shi Xu, Flynn D, Tay B K, Prawer S, Nugent K W, Silva S R P, Lifshitz Y and Milne W I 1997 *Phil. Mag.* B **76** 351
[7] Oguri K and Arai T 1996 *J. Mater. Res.* **5** 2567
Oguri K and Arai T 1992 *Thin Solid Films* **208** 158
[8] Gangopadhyay A K, Willermet P A, Tamor M A and Vassell W C 1997 *Tribol. Int.* **30** 9
[9] De Martino C, Fusco G, Mina G, Tagliaferro A, Vanzetti L, Calliari L and Anderle M 1997 *Diamond Relat. Mater.* **6** 559
[10] Chhowalla M, Yin Y, Amaratunga G A, McKenzie D R and Frauenheim T 1996 *Appl. Phys. Lett.* **69** 2344
[11] Cheah L K, Shi X, Shi J R, Liu E J and Silva S R P 1998 *J. Non-Cryst. Solids* **242** 40
[12] Shi X, Flynn D, Tay B K and Tan H S 1995 Filtered cathodic arc source *GB Patent Specification* PCT/GB96/00389
[13] Shi X, Fulton M, Flynn D, Tay B K and Tan H S 1995 Deposition apparatus *GB Patent Specification* PCT/GB96/00390
[14] Moulder J F, Stickle W F, Sobol P E and Bomber K D 1992 *Handbook of X-ray Photoelectron Spectroscopy* ed J Chastain (Eden Prairie, MN: Perkin-Elmer)
[15] Bradley R M 1989 *Handbook of Ion Beam Processing Technology, Principles, Deposition, Film Modification and Synthesis* ed J J Cuomo, S M Rossnagel and H R Kaufman (Park Ridge, NJ: Noyes) p 300
[16] Shi X, Cheah L K, Shi J R, Sun Z and Tay B K 1999 *J. Phys.: Condens. Matter* **11** 185
[17] Tay B K, Shi X, Tan H S, Yang H S and Sun Z 1998 *Surf. Coatings Technol.* **105** 155
[18] Zhang X, Weber W H, Vassell W C, Potter T J and Tamor M A 1998 *J. Appl. Phys.* **83** 2820
[19] Kumbhar A S, Bhusari D M and Kshirsagar S T 1995 *Appl. Phys. Lett.* **66** 1741
[20] Smith J E, Brodsky M H, Crowder B L, Nathan M I and Pinczuk A 1971 *Phys. Rev. Lett.* **26** 642
[21] Morell G, Katiyar R S, Weisz S Z and Balberg I 1996 *J. Non-Cryst. Solids* **194** 78
[22] Prawer S, Nugent K W, Lifshitz Y, Lempert G D, Grossman E, Kulik J, Avigal I and Kalish R 1996 *Diamond Relat. Mater.* **5** 433
[23] Gilkes K W R, Sands H S, Batchelder D N, Robertson J and Milne W I 1997 *Appl. Phys. Lett.* **70** 1980
[24] Sun Z, Sun Y, Wang X and Zheng Z 1995 *Mater. Sci. Eng.* B **34** L13